A&A, 707, A205 (2026)
https://doi.org/10.1051/0004-6361/202557111

Astronomy & Astrophysics

Apsidal motion and TESS light curves of two southern eclipsing binaries with high eccentricity: V1647 Sgr and V2283 Sgr

M. Wolf[1,⋆], P. Zasche[1], M. Zejda[2], and M. Mašek[3,4]

[1] Astronomical Institute, Faculty of Mathematics and Physics, Charles University Prague, V Holešovičkách 2, CZ-180 00 Praha 8, Czech Republic
[2] Department of Theoretical Physics and Astrophysics, Masaryk University,Kotlářská 2, CZ-611 37 Brno, Czech Republic
[3] FZU - Institute of Physics of the Czech Academy of Sciences, Na Slovance 1999/2, CZ-182 21 Praha 8, Czech Republic
[4] Czech Astronomical Society, Variable Star and Exoplanet Section, Vídeňská 1056, CZ-142 00 Praha 4, Czech Republic

Received 5 September 2025 / Accepted 30 January 2026

ABSTRACT

The study of apsidal motion rates in eccentric eclipsing binaries provides an important observational test of theoretical models of stellar structure and evolution. Precise physical parameters of the stellar components together with systematic measurements of the periastron advance are needed. We present new results of our long-term observational project to analyze the apsidal motion in early-type eccentric eclipsing binaries. New ground- and space-based photometric data were obtained, and archival spectroscopic measurements were used in this study of two detached southern hemisphere eclipsing binaries: V1647 Sgr ($P = 3^{\rm d}.28, e = 0.41$), and V2283 Sgr ($3^{\rm d}.47, 0.49$). Their TESS observations in four sectors were also included, and the corresponding light curves were solved using the code PHOEBE. The newly completed $O - C$ diagrams were analyzed using all reliable timings found in the literature and calculated using the TESS light curves. New or improved values were obtained for the elements of apsidal motion. Using archival spectroscopy for V1647 Sgr, we improved the precise absolute parameters to $M_1 = 2.184(0.035)\,M_\odot$, $M_2 = 1.957(0.035)\,M_\odot$, and $R_1 = 1.839(0.015)\,R_\odot$, $R_2 = 1.716(0.015)\,R_\odot$. For V2283 Sgr, the absolute dimensions were newly estimated to $M_1 = 2.178(0.10)\,M_\odot$, $M_2 = 1.547(0.10)\,M_\odot$, and $R_1 = 1.796(0.01)\,R_\odot$, $R_2 = 1.544(0.01)\,R_\odot$. We improved relatively long periods of apsidal motion of about 580 and 530 years, together with the corresponding internal structure constants, log k_2, –2.394, and –2.418, for V1647 Sgr and V2283 Sgr, respectively. The relativistic contribution to apsidal motion is not negligible. It is about 12 and 14% of the total rate of apsidal motion for V1647 Sgr and V2283 Sgr, respectively. No signs of an additional body were revealed in the light curves or in the $O - C$ diagrams of the two eccentric systems.

Key words. binaries: close – binaries: eclipsing – stars: early-type – stars: fundamental parameters – stars: individual: V1647 Sgr – stars: individual: V2283 Sgr

1. Introduction

Some bright stellar objects still escape current efforts of studying them, but they are of fundamental importance for a broader astrophysical context in stellar astrophysics. One such group is that of eccentric eclipsing binaries (EEBs), which provides an ideal opportunity to verify stellar structure and to test General Relativity effects outside the Solar System (Giménez 2007; Claret & Giménez 2010; Claret & Torres 2019). Moreover, detached double-line eclipsing binaries (DLEBs) simultaneously serve as an important source of fundamental information on stellar masses and radii (Andersen 1991). Torres et al. (2010) revised the absolute dimensions of 94 DLEBs and found that only 18 have eccentric orbits with an apsidal motion that is suitable for the apsidal motion test of the stellar structure.

An analysis of apsidal motion in eclipsing binaries using Transiting Exoplanet Survey Satellite (TESS) data was recently presented by Baroch et al. (2021, 2022). These authors determined the apsidal motion rate for 9 EEBs, measured the general relativistic apsidal motion rate, and performed a test of General Relativity. They found perfect agreement with theoretical predictions and established stringent constraints on the parameters of the post-Newtonian formalism. Recently, Claret et al. (2021) studied the internal structure constant (ISC) in 34 EEBs and nearly doubled the sample of suitable systems collected by Torres et al. (2010). They show that the apsidal motion rate is in agreement with predictions based on new theoretical models. Therefore, it is necessary to expand the current collection of EEBs with precise absolute parameters to provide better statistics on these results. The only exception is EM Car, with the highest mass of both components ($22.8 + 21.4\,M_\odot$). This object deserves further attention (Claret et al. 2021).

However, a precise determination of the apsidal motion rate requires long-term monitoring of mid-eclipse times, usually spanning several decades, and many advanced amateur observers can help with this difficult task. Apsidal motion studies and the determination of precise stellar parameters remain the subject of many papers. We recall the extensive studies of Hong et al. (2016) and Zasche et al. (2020) or recent works on individual objects (Southworth 2024; Kozyreva et al. 2024; Zasche et al. 2024; Volkova & Volkov 2025). The apsidal motion rate can also be determined with relatively good precision in spectroscopic binaries of the SB2 type, for which the radial velocities of the primary and secondary components are measured over a long time interval (Schmitt et al. 2016; Rauw et al. 2016) by changes in the shape of the light curve over time (Harmanec et al. 2014; Torres et al. 2017), or even by combining photometry and spectroscopy (Rosu et al. 2020, 2022a,b).

⋆ Corresponding author: marek.wolf@mff.cuni.cz

Table 1. Properties of the two selected EEBs.

System	HD number	CD number	Spectral type	Period [day]	V [mag]	$B-V$ [mag]	G [mag]	Parallax [mas]	Eccentricity –
V1647 Sgr	HD 163708	CD-36 12064	A1V	3.283	7.09	0.066	7.071	6.01	0.412
V2283 Sgr	HD 321230	CD-36 12180	A0V	3.471	10.4	0.06	10.282	1.62	0.489

Notes. The spectral type, V and G magnitudes, and parallax values are taken from the SIMBAD database.

The two binary systems we studied have many similarities and common characteristics: a rather longer orbital period of about 80 hours, an early spectral type A, a high orbital eccentricity (more than 0.4), a slow apsidal motion with a similar period of over 500 years, and finally, their close position in the southern sky in the Sagittarius constellation (about two diameters of the Moon apart). We recall that the (likely) highest known eccentricity of $e = 0.618$ was discovered in the eclipsing binary V680 Mon by Volkov et al. (2021). Basic properties of V1647 Sgr and V2283 Sgr are summarized in Table 1. This study of apsidal motion in EEBs is a continuation of the work we presented in earlier papers over several decades, the last time in Wolf et al. (2022, 2024). The current paper is organized as follows. Section 2 presents new observations and data reductions. We analyze the apsidal motion in Sect. 3, and the light curves are analyzed in Sect. 4. The ISCs are calculated in Sect. 5 , and a brief summary of the results is presented in Sect. 6.

The DLEB V1647 Sgr (also HD 163708, $V_{\rm max} = 7.09$ mag) is a bright A-type binary with a high orbital eccentricity ($e = 0.41$). It is located in the vicinity of the bright G8 giant star HD 163652 ($V = 5.7$ mag). Since its discovery by J. Herschel, V1647 Sgr is known as the primary component of the visual double star HJ 5000A. It was discovered to be a variable star by Ponsen (1956) and was independently studied by de Kort (1955). The complete simultaneous Stromgren four-color photometry of V1647 Sgr was obtained in 1973-74 and 1982 at ESO in Chile (Clausen et al. 1977). The spectroscopic orbital elements and absolute dimensions were determined later by Andersen & Gimenez (1985). They also derived an apsidal motion with a period of $U = 592.5 \pm 6.5$ yr and a substantial value for the orbital eccentricity of $e = 0.4130$. They derived the following linear ephemeris:

$$\text{Pri. Min.} = \text{HJD } 24\,41829.69510(1) + 3\overset{\text{d}}{.}28279251(1) \cdot E,$$
$$\text{Sec. Min.} = \text{HJD } 24\,41830.55561(8) + 3\overset{\text{d}}{.}28282227(33) \cdot E.$$

Wolf (2000) studied the apsidal motion and confirmed the parameters derived earlier, with a rather shorter apsidal motion period $U = 531 \pm 5$ years. V1647 Sgr was included in the recent study of Claret et al. (2021), where the observed and theoretical ISCs of 27 EEBs were compared. The observed ISC agrees very well with the predictions based on new theoretical models. For V1647 Sgr, the authors found $\log k_{2,\rm obs} = -2.373$ and $\log k_{2,\rm theo} = -2.384$, which shows that theory and observation agree well.

V1647 Sgr was also incorporated into the study of Kołaczek-Szymański et al. (2021) of the so-called heartbeat stars, which are eccentric binaries with a characteristic shape of their brightness changes close to the periastron passage that is primarily caused by a variable tidal distortion of the components. Dimoff & Orosz (2023) included this object in a sample of 15 EEBs known for their apsidal motion. They compared the derived apsidal rates with an analytic solution and found that they agreed well.

In contrast, the detached eclipsing binary V2283 Sgr (also known as HD 321230, $V_{\rm max} = 10.4$ mag; Sp. A0) is a photometrically and spectroscopically neglected binary with a remarkably eccentric orbit ($e = 0.49$) and a period of about 3.5 days. It was discovered to be a variable by Henrietta Swope on photographic plates in MWF 187 (Shapley & Swope 1938). Kooreman (1965) rediscovered this star in the region around Boss 4599 and found a very high orbital eccentricity of at least 0.45. The first photoelectric observations she obtained by Swope (1974) at the Siding Spring observatory in Australia in 1965, where she derived the following linear light elements:

$$\text{Pri. Min.} = \text{HJD } 24\,38948.5043 + 3\overset{\text{d}}{.}4714231 \cdot E,$$
$$\text{Sec. Min.} = \text{HJD } 24\,38946.7619 + 3\overset{\text{d}}{.}4714231 \cdot E,$$

and the substantial value of $e = 0.49$ for the orbital eccentricity. Swope also found an apsidal motion with a period of $U = 570$ years. Independently, O'Connell (1974) derived similar results, an eccentricity of 0.487 and an apsidal motion period of 560 years. Finally, Wolf (2000) confirmed the parameters mentioned above with a rather shorter apsidal motion period of $U = 528 \pm 12$ years. This binary has rarely been investigated since its discovery, and no spectroscopic observations have been published for this system as far as we know.

Our last study of these two southern EEBs (Wolf 2000) was presented 25 years ago, so we decided to recalculate the apsidal motion with newly available data. In particular, very precise measurements from the TESS satellite are available, and we have a number of new mid-eclipse times that were obtained at several southern observatories.

2. Observations

2.1. Ground-based photometry

Our new photoelectric and CCD observations were obtained at four southern observatories in the past. We describe them below in chronological order.

- South African Astronomical Observatory (SAAO), Sutherland, South Africa. The 0.50 m Cassegrain reflector ($f/18$) is equipped with a modular photometer using a Hamamatsu EA1516 photomultiplier and Johnson UBV filters in September 2005. For the bright V1647 Sgr, a neutral density filter ND1 was included. Alternatively, a Helios 2/58 objective with an ATIK 16 IC CCD camera was used during two weeks in November 2008 and April 2010. The Helios 2/58 objective with a G2-402 CCD camera (BVR filters) was also used in March 2018.
- La Silla Observatory in Chile. The Danish 1.54 m reflecting telescope, the EFOSC camera, and the Johnson B filter were used in remote control during one night on February 17, 2016.
- Fotometric Robotic Atmospheric Monitor (FRAM; Aab et al. 2021), Pierre Auger Observatory, Argentina.

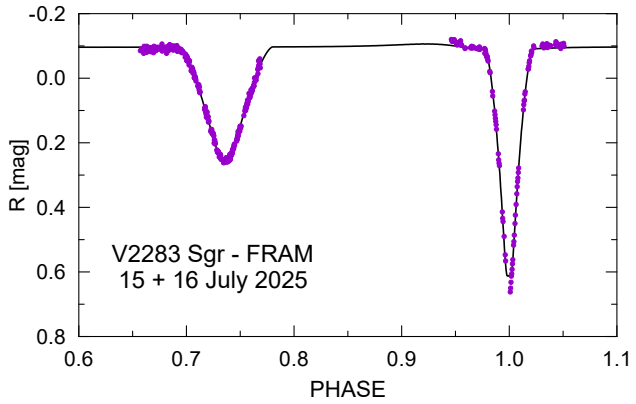

Fig. 1. Example of our photometric observations of V2283 Sgr obtained at the FRAM observatory, Argentina, during two consecutive nights in July 2025. We show differential photometry in *R* filter and its fit in PHOEBE. The secondary minimum of V2283 Sgr falls close to phase 0.75.

The telephoto lens Nikkor 300 mm ($f/2.8$), the CCD camera G4-16000, and the attenuating filter or the ODK 0.30 m telescope ($f/6.8$), the CCD camera G4-16000, and the *R* filter were used in remote control during two epochs in May/August 2020 and July 2025.

– Boyden Observatory, South Africa. The reflecting telescope Celestron CGE 1400 XLT (350/2250), the C3-26000Pro CMOS camera, and the Sloan *gri* filters were used in remote control during several nights in June 2025.

The main aim of these photometric measurements was to secure several well-covered primary and secondary eclipses for both variables. Each observation of an eclipsing binary was accompanied by the observation of local comparison and check stars (see Table A.1).

Photoelectric measurements at SAAO were usually performed using Johnson's *UBV* photometric filters with a 10-second integration time. All observations were carefully reduced to the Cousins E region standard system (Menzies et al. 1989) and corrected for differential extinction using the reduction program HEC 22 rel. 16 (Harmanec & Horn 1998). The standard errors of the *UBV* measurements at SAAO were 0.011, 0.008, and 0.007 mag in the U, B, and V filters, respectively. The C-MUNIPACK[1] software package for aperture photometry, based on the DAOPHOT procedure, was used to process the set of CCD frames. An example of our photometric observations of V2283 Sgr obtained at the FRAM observatory in July 2025 is given in Fig. 1.

2.2. TESS photometry

Moreover, the TESS mission to study exoplanets through photometric transits (Ricker et al. 2015), with its nearly full sky coverage, also provides precise photometry of a large sample of eclipsing binary systems with a time baseline of 27 days to several years. Thus, the precise monitoring of light curves is possible from space, and their exceptional quality is perfect for studying light curves and eclipse timings (Baroch et al. 2021). The two systems we studied were observed by TESS in four identical sectors during 2019–2025 (see Table 2). For V1647 Sgr and V2283 Sgr, we collected simple aperture photometry (SAP) of the available cadence produced by the Science Process Operation Centre (SPOC; Jenkins et al. 2016) available at the Mikulski Archive for Space Telescopes (MAST)[2].

Table 2. Common TESS visibility of V1627 Sgr and V2283 Sgr and sectors used to analyze the light curve and determine the mid-eclipse time.

Sector No.	Start date YYYY-MM-DD	Exposure time [s]
13	2019-06-19	1800
39	2021-05-27	600
66	2023-06-02	200
93	2025-06-03	158

The pixels of the TESS detectors cover a sky area of 21×21 arcsec. The TESS aperture photometry is extracted over several pixels, and we thus checked *Gaia* Data Release 3 (DR3; Gaia Collaboration 2022) for possible contamination of our objects. The catalog lists up to a thousand objects (in Sgr), all of which are significantly fainter than our targets. The brightest nearby star of V1647 Sgr is the dominant close visual companion HD 163708B, which is fainter by ~2 mag. In the vicinity of V2283 Sgr lies a 3 mag fainter star, Gaia DR3 4037120519350665472. Hence, formally, we included the third light in our PHOEBE solution to reduce contamination from nearby sources.

The new times of primary and secondary minima and their errors were determined using a least-squares fit of the light curve during eclipses. We applied third- and fourth-order polynomial fittings to the bottom sections of the light curves, and the mean value was adopted as the mid-eclipse time. Where needed, the mean values of the individual filter bands are given, and the errors represent the fitting mean error for each light curve. For the TESS data, the mid-eclipse times were determined using the code SILICUPS[3]. Because the TESS data are provided in the barycentric Julian date dynamical time (BJD_{TDB}), all our previous times were first transformed to this time scale using the often used code called time utilities of Ohio State University[4] (Eastman et al. 2010). All new minima times for V1647 Sgr and V2283 Sgr in BJD are collected in Tables A.2 and A.3, and the epochs were calculated from the light ephemeris given in the text.

2.3. ASAS-3, OMC, and Pi of the Sky photometry

Using the All Sky Automated Survey-3 (ASAS-3) database[5] (Pojmanski 2002), photometric data from the INTEGRAL Optical Monitoring Camera Archive (OMC) (Mas-Hesse et al. 2004)[6], and Pi of the Sky (Burd et al. 2005), we were able to derive several additional times of minimum light with a precision of about 0.001–0.002 days. They were used in our analysis below with a weight of 1.

To derive some of the eclipse times from various surveys with sparse photometry, we used our semi-automatic fitting

[1] Motl, 2018, https://c-munipack.sourceforge.net/, ver. 2.1.24.

[2] https://mast.stsci.edu/portal/Mashup/Clients/Mast/Portal.html

[3] SImple LIght CUrve Processing System, https://www.gxccd.com/cat?id=187&lang=405

[4] http://astroutils.astronomy.ohio-state.edu/time/

[5] http://www.astrouw.edu.pl/asas/

[6] https://sdc.cab.inta-csic.es/omc/

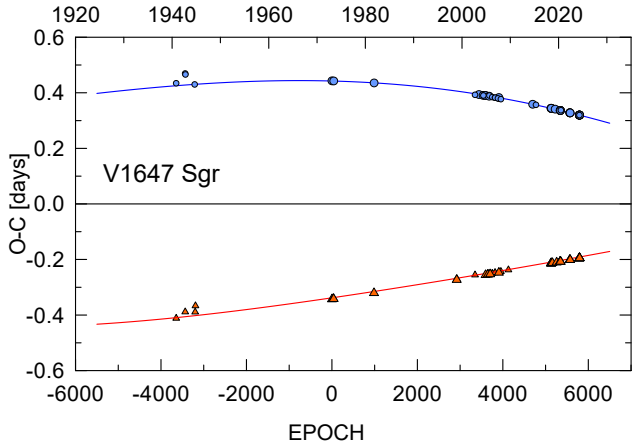

Fig. 2. Complete $O - C$ diagram of V1647 Sgr spanning almost one century. Primary minima are denoted by blue circles, and secondary minima by orange triangles. The curves correspond to our best-fit apsidal motion model. All TESS data represent four clusters of points at the end of the two curves.

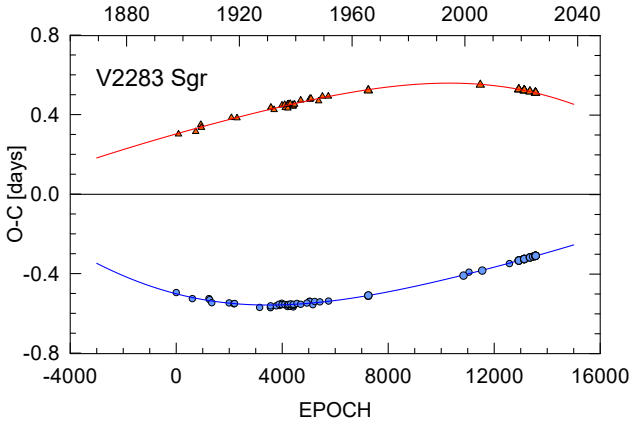

Fig. 3. Historical $O - C$ diagram of V2283 Sgr since the beginning of the 20th century, together with our best-fit apsidal motion model. See the legend to Fig. 2.

procedure (AFP, described in Zasche et al. (2014)). It uses the phased light curve over a longer time interval and the template of the light curve provided through light curve modeling in PHOEBE. The time interval we used was typically one year, but this can be arbitrarily changed with respect to the number of data points in each interval. We are typically able to derive several times of eclipses, primary and secondary, using this method from one particular photometric survey dataset.

2.4. Spectroscopy

The previously published spectroscopy and radial velocity curve are only available for V1647 Sgr (Andersen & Gimenez 1985, their Table 2). A total of 27 spectrograms were obtained at the 1.5 m ESO telescope and coudé spectrograph at La Silla, Chile, in two consecutive seasons in 1976–1977. We used this precise and compact dataset for a common solution in PHOEBE. To our knowledge, no spectroscopic material or radial velocities have been reported in the literature for the relatively bright target V2283 Sgr, nor in any available electronic database.

3. Apsidal motion analysis

The study of apsidal motion requires long-term monitoring of eclipse times, usually spanning several decades. This is not an observing program that requires large telescopes, but advanced amateur astronomers can help with this time-consuming task. As in our previous studies, apsidal motion was studied using an $O - C$ diagram (or an eclipse time variation) analysis. The iterative method described by Giménez & Garcia-Pelayo (1983) or Giménez & Bastero (1995) was used again. We collected all suitable mid-eclipse times available in the literature and current databases. The input files of the minima were completed with our own measurements and all available data from TESS. All photoelectric and CCD times and the TESS minima were used with a weight of 10 in our calculation. Previous less accurate measurements with unknown uncertainty (photographic or visual estimates) were assigned weights 1 or 0. However, due to the long time lag and high dispersion of these measurements from the first half of the 20th century, the final solution may depend on the adopted weighting scheme. The apsidal motion parameters were calculated iteratively. For the orbital inclination, we adopted the results of our own photometric solution (see Chapter 4 and Table 4). In contrast, the eccentricity resulting from the analysis of the apsidal motion was fixed in the following solution of the light curves. In general, the apsidal motion solution was found to be insensitive to relatively large changes in inclination but to strongly depend on the orbital eccentricity.

In the case of V1647 Sgr, original photographic times of the minima of Ponsen (1956) and all the photoelectric times given in Clausen et al. (1977) (their Tables 2 and 3) were incorporated into our calculation. Several times with lower precision were found in the literature or were derived using Pi of the Sky and OMC photometry. Our new *VR* CCD photometry obtained at the FRAM and Boyden observatories was also used to determine new mid-eclipse times. A large number of very precise and consecutive times were obtained using the TESS data in four sectors. A total of 94 times of minimum light were used in our analysis and included 48 secondary eclipses. All are listed in Tables A.2 and A.3.

For V2283 Sgr, there is a limited number of new precise electronic mid-eclipse times. All photographic eclipse times given in Shapley & Swope (1938) and O'Connell (1974) were included in our analysis. Four new and precise times were derived using our FRAM and Boyden observations. The most numerous contribution of minima comes from four TESS sectors. The newly determined times of minimum light are listed in Tables A.2 and A.3, where all epochs were computed according to the ephemeris given in the text. In our analysis of V2283 Sgr, a total of 115 times of minimum light were used.

The residuals of $O - C$ values for all minimum times with respect to the linear part of the apsidal motion equation are shown in Figs. 2 and 3. The computed elements of apsidal motion and their internal errors of the least-squares fit are given in Table 3, where $\dot{\omega}$ is the rate of periastron advance (in degrees per cycle or in degrees per year), and the periastron position for the zero epoch T_0 is denoted as ω_0. The relation between the sidereal and the anomalistic period, P_s and P_a, is given by

$$P_s = P_a\,(1 - \dot{\omega}/360^\circ), \tag{1}$$

which means that the sidereal period is always a little shorter than the anomalistic period due to apsidal motion. Finally, the period of apsidal motion is $U = 360^\circ P_a/\dot{\omega}$. The nonlinear predictions, corresponding to the fitted parameters, are plotted as blue and orange curves for the primary and secondary eclipses, respectively.

Table 3. Apsidal motion elements of V1647 Sgr and V2283 Sgr.

Element	Unit	V1647 Sgr	V2283 Sgr
T_0	BJD-2400000	41829.2523(3)	13784.1605(2)
P_s	days	3.28280010(8)	3.47142150(5)
P_a	days	3.28285098(8)	3.47148337(5)
e	–	0.412 (1)	0.489 (1)
$\dot{\omega}_{\rm obs}$	deg cycle^{-1}	0.00557 (7)	0.00642 (8)
$\dot{\omega}_{\rm obs}$	deg yr^{-1}	0.620 (7)	0.675 (8)
ω_0	deg	203.5 (5)	315.8 (5)
U	years	580 (20)	533 (20)
$\Sigma w(O-C)^2$	day^2	$6.7 \cdot 10^{-4}$	$3.0 \cdot 10^{-3}$

Notes. The uncertainties are given in parentheses.

Table 4. Parameters of the fit to the TESS light curve in PHOEBE.

Element	V1647 Sgr	V2283 Sgr
T_1 [K] (fixed)	9600 (300)*	9700 (300) †
T_2 [K]	9000 (300)	7950 (300)
$r_1 = R_1/a$	0.1232 (45)	0.1201 (50)
$r_2 = R_2/a$	0.1150 (45)	0.1033 (50)
e (fixed)	0.412	0.489
i [deg]	89.9 (4)	89.5 (5)
Ω_1	9.645	9.717
Ω_2	8.927	8.986

Notes. * value taken from Torres et al. (2010). † probable value according to the literature.

4. Analysis of the light curve and radial velocity

Because the data obtained at the SAAO, FRAM, and Boyden observatories are less precise and noncontinuous compared to the TESS data, only the TESS light curves were selected to fit the light curves of both systems. The other available photometric data were mostly used to determine the mid-eclipse time and the solution of apsidal motion. The completely covered light curves were routinely analyzed using the code PHOEBE, developed by Prša & Zwitter (2005) (see also Prša (2018)), which is a user-friendly implementation of the traditional Wilson-Devinney code (Wilson & Devinney 1971). However, solving the light curves of eccentric binaries in PHOEBE is a rather challenging and time-consuming task. To reduce the long computation time for eccentric orbits, the TESS light curves were phased-binned to 300 points each.

The light elements, eccentricity, and apsidal motion rate were adopted from the previous apsidal motion analysis (see Sect. 3 and Table 3). The minimum times cover a longer time span, and these quantities are derived with higher precision. The other light-curve parameters were fitted: the luminosities, temperature of the secondary, inclination, and Kopal's modified potentials (Kopal 1959; Wilson 1979). These potentials ($\Omega \sim R^{-1}$) contain contributions from the star, its nearby companion, the star's rotation about its axis, and the star's rotation on its orbit.

Because all components belong to early-type stars, we adopted bolometric albedos and gravity darkening coefficients as $A_1 = A_2 = 1.0$ and $g_1 = g_2 = 1.0$, which correspond to radiative envelopes. We also assumed synchronous rotation for both components ($F_1 = F_2 = 1$). For elliptical orbits, the rotation usually tends to synchronize because of tidal interactions between the two components. The limb-darkening coefficients were interpolated from van Hamme's tables (van Hamme 1993) using the logarithmic law. We also tested the linear cosine limb-darkening law and found little effect on our resulting parameters. For the solution of V1647 Sgr, the radial velocities of Andersen & Gimenez (1985) were used as an important input file. The fine and coarse grid rasters for both components were set to 30. The final solution was accepted when several subsequent iterations did not result in a decrease in the PHOEBE cost function. The results of the photometric analysis are given in Table 4. In this table, T_1, T_2 denotes the temperatures of the primary and secondary components, r_1, r_2 the relative radii, i the orbital inclination, and Ω_1, Ω_2 Kopal's modified potentials. The corresponding light curves are plotted in Figs. 4 and 6, respectively. The TESS phased-binned light curve of both systems shows out-of-eclipse variations caused by light reflection from one component to the other close to periastron, and it is well resolved using the code PHOEBE. The results of the simultaneous analysis of the light curve and the radial velocity curve, and the absolute dimensions for V1647 Sgr are listed in Table 5. The radial velocity curve for V1647 Sgr obtained by Andersen & Gimenez (1985) and its current solution are plotted in Fig. 5.

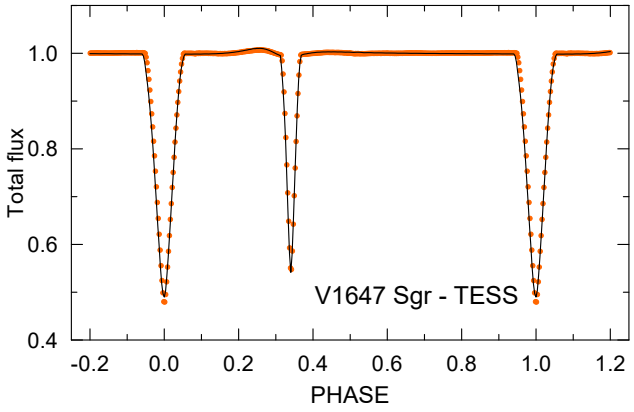

Fig. 4. TESS light curve of V1647 Sgr obtained in Sector 66 (June 2023, orange dots, binning 300) and its PHOEBE solution (black curve).

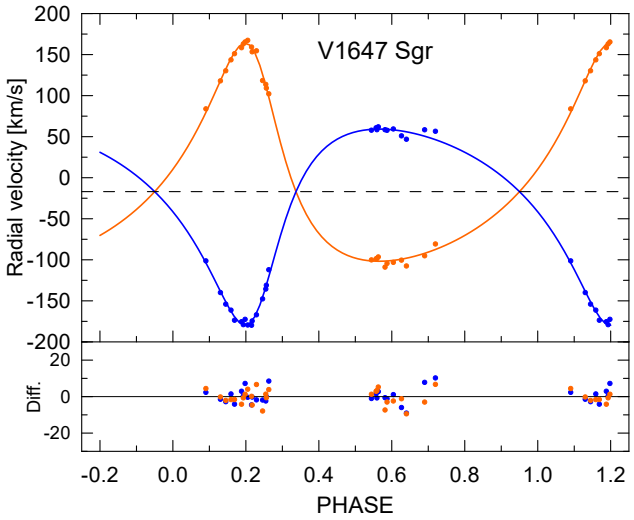

Fig. 5. Radial velocity curve for V1647 Sgr obtained by Andersen & Gimenez (1985) and its current solution in PHOEBE. Blue denotes the primary component, and orange shows the secondary. The γ-velocity (–17 km/s) is plotted as a dotted line. The residuals are given in the bottom panel.

Table 5. Astrophysical parameters and ISCs and their comparison.

Parameter	Unit	V1647 Sgr this paper	V1647 Sgr Torres et al. (2010)	V2283 Sgr this paper
M_1	$M_\odot$	2.184 (35)	2.184 (37)	2.178 (100)
M_2	$M_\odot$	1.957 (35)	1.967 (33)	1.547 (100)
R_1	$R_\odot$	1.839 (15)	1.832 (18)	1.796 (10)
R_2	$R_\odot$	1.716 (15)	1.667 (17)	1.544 (10)
$\log g_1$	cgs	4.248	4.2517 (78)	4.267
$\log g_2$	cgs	4.187	4.2879 (84)	4.250
$q = M_2/M_1$	–	0.899 (12)	0.901 (9)	0.71
a	$R_\odot$	14.92	14.33	15.0
γ	km s^{-1}	–16.97	–16.8	–
$\dot{\omega}_{\rm rel}$	deg cycle^{-1}	0.000 77	–	0.000 75
$\dot{\omega}_{\rm rel}/\dot{\omega}$	%	13.8	–	11.7
$\log k_{2,\rm obs}$	–	–2.394 (25)	–2.373 (19)	–2.418 (30)
$\log k_{2,\rm theo}$	–	–2.384 †	–2.384 (37)	–2.38(4) ‡

Notes. † value taken from Claret et al. (2021). ‡ value interpolated in the models by Claret (2023) for the expected masses and age.

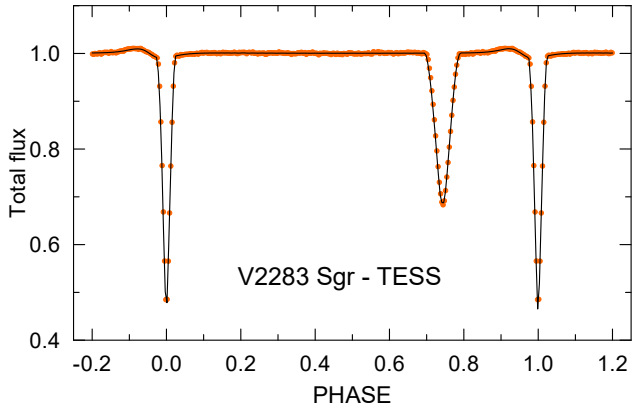

Fig. 6. TESS light curve of V2283 Sgr with remarkable eccentricity obtained in Sector 39 (May/June 2021, orange dots, binning 300) and its PHOEBE solution (black curve).

For V2283 Sgr, different values of the temperature of the primary component can be found: 8944 K from the TESS Input Catalog (Stassun et al. 2019), 9600 K from *Gaia* BP/RP spectra (Verberne et al. 2024), 9700 K from the Modern Mean Dwarf Stellar Color and Effective Temperature Sequence (Pecaut & Mamajek 2013), and 9777 K from *Gaia* DR3 (Gaia Collaboration 2022) We adopted a temperature $T_1 = 9700 \pm 300$ K as a probable value based on these several sources. The spectral type and masses were then interpolated in the table of Pecaut & Mamajek (2013)[7]. The temperature of the secondary and the dimensions of the components were then estimated using the PHOEBE solution. The semimajor axis a in solar radii was computed according to the third Kepler law.

5. Internal structure constant

The great advantage of the detected apsidal motion in binaries is its direct connection with the ISC, k_2, of both components. Generally, the ISC is a measure of the density profile inside the star and is an important additional parameter of stellar evolution models. The mean value of the observed $\bar{k}_{2,\rm obs}$ is given by

$$\bar{k}_{2,\rm obs} = \frac{1}{c_{21}+c_{22}}\frac{P_a}{U} = \frac{1}{c_{21}+c_{22}}\frac{\dot{\omega}_{\rm cl}}{360}, \quad (2)$$

where c_{21} and c_{22} are functions of the orbital eccentricity, fractional radii, masses of the components, and the ratio of the rotational velocity of the stars to the Keplerian velocity (Kopal 1978), and $\dot{\omega}_{\rm cl}$ represents the classical (or Newtonian) contribution to apsidal motion; see below. The rotation of the stars was assumed to be synchronized with the maximum angular orbital velocity achieved at periastron.

The observed ISC is very sensitive to the radii of components ($k_{2,\rm obs} \sim R^5$), and this test can only be performed for systems with accurate radii that provide eclipsing binaries. The theoretical ISC, $k_{2,\rm theo}$, is a combination of the ISC of the two components,

$$k_{2,\rm theo} = \frac{c_{21}k_{21} + c_{22}k_{22}}{c_{21}+c_{22}}, \quad (3)$$

which can be compared with the observational value.

The observed apsidal motion rate has two independent components: the classical (Newtonian) term, due to the nonspherical shape of the two stars, and the relativistic term due to General Relativity effects. Taking into account the value of the eccentricity and the masses of the components, a relativistic term, $\dot{\omega}_{\rm rel}$, must first be subtracted. The original equation of Levi-Civita (1937) can be rewritten to be a more suitable function of the known observable parameters in degrees per cycle (Giménez 1985; Dimoff & Orosz 2023),

$$\dot{\omega}_{\rm rel} = 5.447\times10^{-4}\,\frac{1}{1-e^2}\left(\frac{M_1+M_2}{P}\right)^{2/3}, \quad (4)$$

where M_i denotes the individual masses of the components in solar units, and P is the orbital period in days. It is clear that systems with higher stellar masses and shorter orbital periods will have a larger relativistic apsidal motion. The value of the classical contribution to the observed apsidal motion rate $\dot{\omega}_{\rm cl}$ is then the following:

$$\dot{\omega}_{\rm cl} = \dot{\omega}_{\rm obs} - \dot{\omega}_{\rm rel}. \quad (5)$$

[7] A Modern Mean Dwarf Stellar Color and Effective Temperature Sequence https://www.pas.rochester.edu/~emamajek/EEM_dwarf_UBVIJHK_colors_Teff.txt

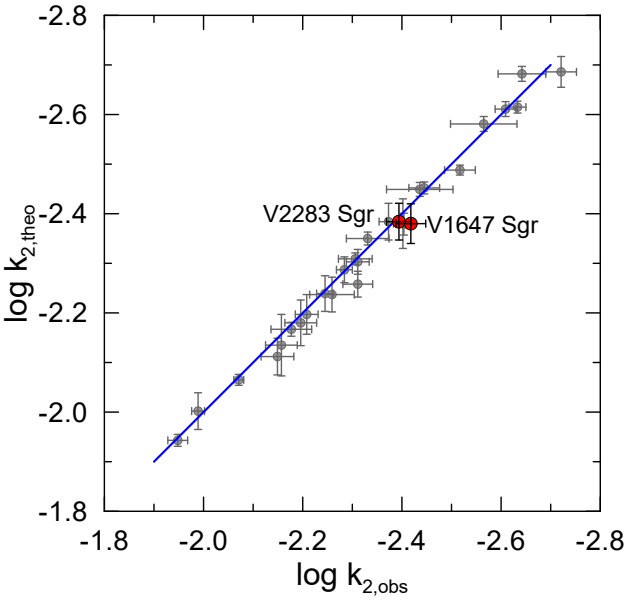

Fig. 7. Comparison of theoretical and observed ISCs for V1647 Sgr and V2283 Sgr (red dots) with other known eccentric systems collected in (Claret et al. 2021, their Table 3).

The astrophysical parameters of both systems are collected in Table 5, as are the values of $\dot{\omega}_{\rm rel}$ and the resulting mean ISCs, $\overline{k}_{2,\rm obs}$. Their errors were determined using the relation derived in Wolf & Zejda (2005).

6. Discussion and conclusions

This study provides actual information on the apsidal motion rates, absolute parameters, and observed ISC values for two close southern EEBs. Our results for apsidal motion and light-curve analyses of V1647 Sgr are similar to the parameters previously derived by Wolf (2000) and Torres et al. (2010). This system consists of two similar stars of spectral type A1. It was also confirmed that V1647 Sgr shows a slow but measurable apsidal motion with a rather long period of about 580 ± 20 years. The masses of both components, $M_1 = 2.184\,M_\odot$ and $M_2 = 1.957\,M_\odot$, were slightly improved. For the primary component of V2283 Sgr, we found almost the same absolute parameters as for the V1647 Sgr primary. The apsidal motion period in this system is somewhat shorter, $U = 533 \pm 20$ years. The secondary component is smaller and cooler. The values obtained for the mean ISC, $\overline{k}_{2,\rm obs}$ were compared with their theoretical values $k_{2,\rm theo}$ according to the current models along the main sequence computed by Claret (2023). The agreement within the given errors can be seen in Fig. 7.

The absolute dimensions of the components of both systems are given in Table 5. The values for V1647 Sgr are sufficiently precise for a comparison with current theoretical models, and its masses and radii are known with an uncertainty of about 1–2%. Their positions in the Hertzsprung-Russell diagram, which contains the evolutionary models for different masses according to Claret (2019), are plotted in Fig. 8. In the bottom part of this figure, the position of the components is compared with the set of isochrones calculated for ages from $2 \cdot 10^8$ to 10^9 years, according to the CMD 3.7 web interface and the PARSEC 2.0 models (Bressan et al. 2012) available on the web pages of the Osservatorio Astronomico di Padova[8]. The common age of all components is assumed to be about $2 \cdot 10^8$ years.

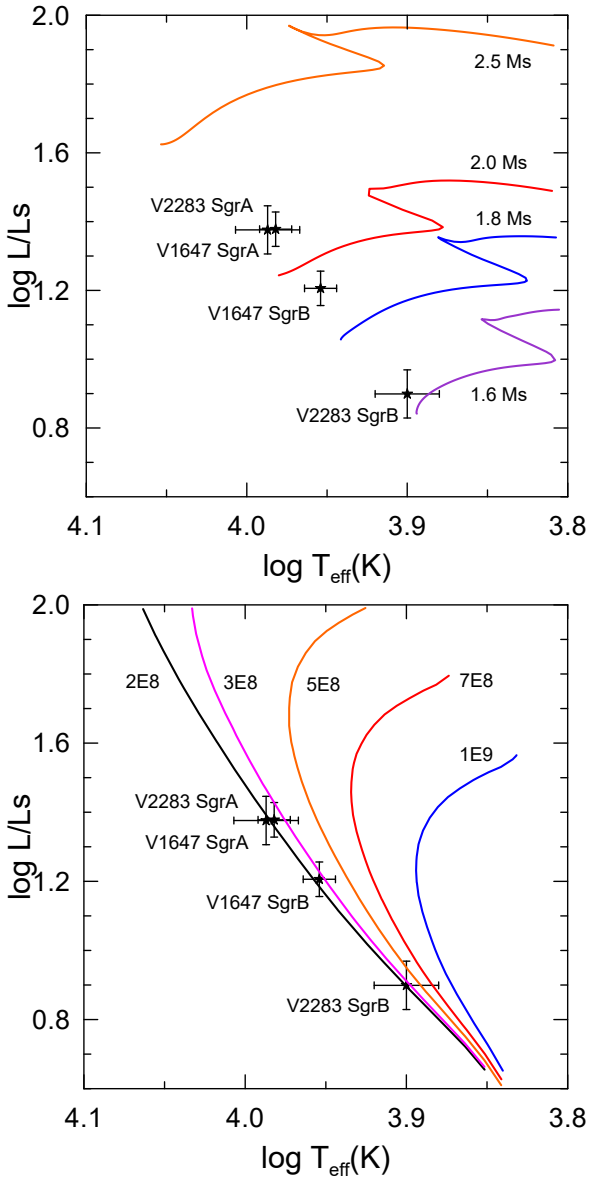

Fig. 8. Hertzsprung-Russell diagram for the binary components. Upper panel: Models of stellar evolution according to Claret (2019) for masses of 1.6, 1.8, 2.0, and $2.5\,M_\odot$. Bottom panel: Isochrones calculated for ages from $2 \cdot 10^8$ to 10^9 yr according to CMD 3.7 and PARSEC 2.0 models. The similarity of the primary components of the two binaries is clearly visible.

Since its discovery, a total of 22 positional measurements of V1647 Sgr have been published. These show only very negligible motion on the sky, indicating a very long orbital period of the pair. Our calculations show that the orbit is probably longer than 1000 years; hence, any significant movement of the double around a common barycenter is undetectable with our data (in the radial velocities of the components, and in $O - C$ of the eclipsing inner pair). Due to its separation on the sky (currently, about 7.5″) and about 2 magnitudes lower brightness, this distant component is not visible in the spectra of V1647 Sgr itself either. These components share the same parallax and similar proper motion (according to the *Gaia* DR3 catalog), and it therefore

[8] http://stev.oapd.inaf.it/cgi-bin/cmd_3.7

probably is a classical hierarchical triple system. The third C component in the Washington Double Star Catalog (WDS) is also very remarkable. This component lies at a distance of about 90″, but its connection to V1647 Sgr is highly speculative. It shares a similar parallax; however, its proper motion is significantly different. Hence, we conclude that this component is probably not connected to V1647 Sgr itself.

The two systems V1647 Sgr and V2283 Sgr are members of an important group of eclipsing binaries with precise absolute dimensions that are suitable for subsequent studies. Although the presence of a close third body is relatively common in eccentric binaries (Wolf et al. 2017, 2022), it has not been demonstrated in these two systems, and no indications of a third component were observed in their $O - C$ diagrams or light curves. In the case of V2283 Sgr, we do not yet know the absolute parameters with great precision. It would also be desirable to obtain new high-dispersion, high-S/N spectroscopic observations to obtain the radial velocity curve and derive accurate masses for this system. We expect radial velocity amplitudes of about 200 km/s.

Acknowledgements. Based on observations secured at the South Africa Astronomical Observatory, Sutherland, South Africa, La Silla Observatory, Chile, FRAM, Pierre Auger Observatory, Argentina, and Boyden Observatory, South Africa. Useful suggestions and recommendations from an anonymous referee helped us improve the clarity of the article and are greatly appreciated. The research of MW and PZ was partially supported by the project COOPERATIO – PHYSICS of Charles University in Prague. This publication was produced within the institutional support framework for the development of the research organization at Masaryk University. This investigation was supported by the allocation of SAAO observation time. We thank the SAAO staff for their warm hospitality and assistance with the equipment. The authors thank Jan Vraštil and Lukáš Pilarčík, former students at Astronomical Institute, Charles University Prague, for their important contribution to photometric observations with the DK154 telescope. This paper includes data collected by the TESS mission. The funding for the TESS mission is provided by the NASA Science Mission Directorate. Data presented in this paper were obtained from the Mikulski Archive for Space Telescopes (MAST). The authors thank the Pierre Auger Collaboration for the use of its facilities. This work is supported by MEYS of Czech Republic under the projects MEYS LM2023032, LM2023047, and CZ.02.01.01/00/22_008/0004632. The operation of the FRAM robotic telescope is supported by the grant from the Ministry of Education of the Czech Republic LM2018102. The data calibration and analysis related to the FRAM telescope is supported by the Ministry of Education of the Czech Republic MSMT-CR LTT18004, MSMT/EU funds CZ.02.1.01/0.0/0.0/16_013/0001402, CZ.02.1.01/0.0/0.0/18_046/0016010 and CZ.02.1.01/0.0/0.0/18_046/0016007. The following Internet-based resources were used in the research for this paper: the SIMBAD database (Wenger et al. 2000) and the VizieR catalog access tool (Ochsenbein et al. 2000), operated at CDS, Strasbourg Astronomical Observatory, France, NASA's Astrophysics Data System Bibliographic Services, the OMC Archive at LAEFF, preprocessed by ISDC, and the VarAstro (`https://var.astro.cz/en/`), a portal for sharing photometric data by the Variable Star and Exoplanet Section, Czech Astronomical Society. This investigation is also part of an ongoing collaboration between professional astronomers and the Czech Astronomical Society, Variable Star and Exoplanet Section.

References

Aab, A., Abreu, P., Aglietta, M., et al. 2021, J. Instrum., 16, P06027
Andersen, J. 1991, A&ARv, 3, 91
Andersen, J., & Gimenez, A. 1985, A&A, 145, 206
Baroch, D., Giménez, A., Ribas, I., et al. 2021, A&A, 649, A64
Baroch, D., Giménez, A., Morales, J. C., et al. 2022, A&A, 665, A13
Bressan, A., Marigo, P., Girardi, L., et al. 2012, MNRAS, 427, 127
Burd, A., Cwiok, M., Czyrkowski, H., et al. 2005, New Astron., 10, 409
Claret, A. 2019, A&A, 628, A29
Claret, A. 2023, A&A, 674, A67
Claret, A., & Giménez, A. 2010, A&A, 519, A57
Claret, A., & Torres, G. 2019, ApJ, 876, 134
Claret, A., Giménez, A., Baroch, D., et al. 2021, A&A, 654, A17
Clausen, J. V., Gyldenkerne, K., & Gronbech, B. 1977, A&A, 58, 121
de Kort, J. J. M. A. 1955, Ric. Astron., 3, 277
Dimoff, A. J., & Orosz, J. A. 2023, AJ, 166, 114
Dvorak, S. W. 2004, Inf. Bull. Var. Stars, 5542, 1
Eastman, J., Siverd, R., & Gaudi, B. S. 2010, PASP, 122, 935
Gaia Collaboration. 2022, VizieR Online Data Catalog: I/355
Giménez, A. 1985, ApJ, 297, 405
Giménez, A. 2007, in Binary Stars as Critical Tools & Tests in Contemporary Astrophysics, eds. W. I. Hartkopf, P. Harmanec, & E. F. Guinan, 240, 290
Giménez, A., & Bastero, M. 1995, Ap&SS, 226, 99
Giménez, A., & Garcia-Pelayo, J. M. 1983, Ap&SS, 92, 203
Harmanec, P., & Horn, J. 1998, J. Astron. Data, 4, 5
Harmanec, P., Holmgren, D. E., Wolf, M., et al. 2014, A&A, 563, A120
Hong, K., Lee, J. W., Kim, S.-L., Koo, J.-R., & Lee, C.-U. 2016, MNRAS, 460, 650
Jenkins, J. M., Twicken, J. D., McCauliff, S., et al. 2016, SPIE Conf. Ser., 9913, 99133E
Kim, C. H., Kreiner, J. M., Zakrzewski, B., et al. 2018, ApJS, 235, 41
Kołaczek-Szymański, P. A., Pigulski, A., Michalska, G., Moździerski, D., & Różański, T. 2021, A&A, 647, A12
Kooreman, C. J. 1965, Annalen van de Sterrewacht te Leiden, 22, 91
Kopal, Z. 1959, Close Binary Systems (London: Chapman & Hall)
Kopal, Z. 1978, Dynamics of Close Binary Systems (Dordrecht: Reidel)
Kozyreva, V. S., Bogomazov, A. I., & Khamrakulov, F. B. 2024, Peremennye Zvezdy, 44, 131
Levi-Civita, T. 1937, Am. J. Math., 59, 225
Mas-Hesse, J. M., Giménez, A., Domingo, A., et al. 2004, ESA SP, 552, 729
Menzies, J. W., Cousins, A. W. J., Banfield, R. M., & Laing, J. D. 1989, South Afr. Astron. Obs. Circ., 13, 1
Ochsenbein, F., Bauer, P., & Marcout, J. 2000, A&AS, 143, 23
O'Connell, D. J. K. 1974, Ric. Astron., 8, 491
Ogloza, W., Niewiadomski, W., Barnacka, A., et al. 2008, Inf. Bull. Var. Stars, 5843, 1
Paschke, A. 2010, Open Eur. J. Var. Stars, 130, 1
Paschke, A. 2017, Open Eur. J. Var. Stars, 181, 1
Pavlov, H., Mallama, A., Loader, B., & Kerr, S. 2016, JAAVSO, 44, 26
Pecaut, M. J., & Mamajek, E. E. 2013, ApJS, 208, 9
Pojmanski, G. 2002, Acta Astron., 52, 397
Ponsen, J. 1956, Bull. Astron. Inst. Netherlands, 12, 338
Prša, A. 2018, Modeling and Analysis of Eclipsing Binary Stars; The theory and design principles of PHOEBE (Bristol, UK: IOP Publishing)
Prša, A., & Zwitter, T. 2005, ApJ, 628, 426
Rauw, G., Rosu, S., Noels, A., et al. 2016, A&A, 594, A33
Ricker, G. R., Winn, J. N., Vanderspek, R., et al. 2015, J. Astron. Telesc. Instrum. Syst., 1, 014003
Rosu, S., Rauw, G., Conroy, K. E., et al. 2020, A&A, 635, A145
Rosu, S., Rauw, G., Farnir, M., Dupret, M.-A., & Noels, A. 2022a, A&A, 660, A120
Rosu, S., Rauw, G., Nazé, Y., Gosset, E., & Sterken, C. 2022b, A&A, 664, A98
Schmitt, J. H. M. M., Schröder, K.-P., Rauw, G., et al. 2016, A&A, 586, A104
Shapley, H., & Swope, H. H. 1938, Harvard College Obs. Bull., 909, 5
Southworth, J. 2024, Observatory, 144, 278
Stassun, K. G., Oelkers, R. J., Paegert, M., et al. 2019, AJ, 158, 138
Swope, H. H. 1974, Ric. Astron., 8, 481
Torres, G., Andersen, J., & Giménez, A. 2010, A&ARv, 18, 67
Torres, G., McGruder, C. D., Siverd, R. J., et al. 2017, ApJ, 836, 177
van Hamme, W. 1993, AJ, 106, 2096
Verberne, S., Koposov, S. E., Rossi, E. M., et al. 2024, A&A, 684, A29
Volkov, I. M., Kravtsova, A. S., & Chochol, D. 2021, Astron. Rep., 65, 184
Volkova, A. S., & Volkov, I. M. 2025, Astron. Rep., 69, 480
Wenger, M., Ochsenbein, F., Egret, D., et al. 2000, A&AS, 143, 9
Wilson, R. E. 1979, ApJ, 234, 1054
Wilson, R. E., & Devinney, E. J. 1971, ApJ, 166, 605
Wolf, M. 2000, A&A, 356, 134
Wolf, M., & Zejda, M. 2005, A&A, 437, 545
Wolf, M., Zasche, P., Kučáková, H., et al. 2017, Acta Astron., 67, 257
Wolf, M., Zejda, M., Mašek, M., et al. 2022, New Astron., 92, 101708
Wolf, M., Zasche, P., Kára, J., et al. 2024, A&A, 690, A231
Zasche, P. 2010, Inf. Bull. Var. Stars, 5931, 1
Zasche, P., Wolf, M., Vraštil, J., et al. 2014, A&A, 572, A71
Zasche, P., Wolf, M., Kučáková, H., et al. 2020, A&A, 640, A33
Zasche, P., Henzl, Z., & Wolf, M. 2024, A&A, 683, A158

Appendix A: Observations and mid-eclipse times

Table A.1. Selected local comparison and check stars at different observatories.

Variable	Comparison & Check stars	V [mag]	Used for photometry
V1647 Sgr	HD 162926*	6.053	PEP at SAAO in 2004-5 and 2019
	HD 164245*	6.296	PEP at SAAO in 2004-5
	UCAC4 263-150753 †	7.182	CCD at FRAM in 2020
	UCAC4 264-142401	8.340	CCD at FRAM in 2021
	UCAC4 266-143028	10.34	CCD at Boyden in 2025
V2283 Sgr	HD 321231	10.51	CCD at La Silla in 2017
	UCAC4 266-150561	10.69	CCD at Boyden and FRAM in 2025
	UCAC4 266-149980	11.50	CCD at Boyden in 2025
	UCAC4 266-150489	10.73	CCD at FRAM in 2025

Notes. * used also by Clausen et al. (1977). † suspected of variability.

Table A.2. New ground-based times of primary and secondary eclipses of V1647 Sgr and V2283 Sgr.

BJD – 24 00000	Primary/ Secondary	Epoch	Error [day]	Observatory Source
		V1647 Sgr		
53122.47841*	P	3440.0	0.0001	SAAO
53444.1898	P	3538.0	0.001	Pi of the Sky
53631.30885*	P	3595.0	0.0001	SAAO
53632.30894*	S	3595.5	0.0001	SAAO
53809.58157	S	3649.5	0.0004	Zasche (2010)
53903.77889	P	3678.0	0.0005	Pi of the Sky
53983.5713	S	3702.5	0.0010	Ogloza et al. (2008)
53983.5693	S	3702.5	0.001	VarAstro
54353.51691	P	3815.0	0.002	Pi of the Sky
54354.52841	S	3815.5	0.002	Pi of the Sky
54652.25246	P	3906.0	0.0005	ASAS
54653.26823	S	3906.5	0.0005	ASAS
55385.338	S	4129.5	0.004	Paschke (2010)
57248.92319	P	4697.0	0.0002	Pavlov et al. (2016)
57501.69678	P	4774.0	0.002	Paschke (2017)
58681.29755*	S	5133.5	0.001	SAAO
58763.36898	S	5158.5	0.0005	OMC
58975.65853	P	5223.0	0.001	FRAM
59091.65077	S	5258.5	0.001	FRAM
59415.54980	P	5357.0	0.0002	FRAM
60840.26754*	P	5791.0	0.0001	Boyden
60841.39834*	S	5791.5	0.0001	Boyden
		V2283 Sgr		
52132.5608	P	11047.0	0.001	Dvorak (2004)
53617.53614	S	11474.5	0.0001	Kim et al. (2018)
53868.27954	P	11547.0	0.0001	Kim et al. (2018)
57436.936	P	12575.0	0.005	La Silla
60533.47890*	P	13467.0	0.0001	Boyden
60821.61022*	P	13550.0	0.0001	Boyden
60872.76733	S	13564.5	0.0001	FRAM
60873.68241	P	13565.0	0.0001	FRAM

Notes. * mean value of *UBV, VR, VI,* or *gri* measurements.

Table A.3. New TESS times of primary and secondary eclipses of V1647 Sgr and V2283 Sgr derived in individual sectors.

TESS Sector	BJD – 24 00000	Epoch	BJD – 24 0000	Epoch
	V1647 Sgr		V2283 Sgr	
13	58660.51266	5127.0	58658.01711	12926.5
	58661.60068	5127.5	58658.89177	12927.0
	58663.79562	5128.0	58661.48825	12927.5
	58664.88317	5128.5	58662.36318	12928.0
	58676.92638	5132.0	58664.95986	12928.5
	58678.01469	5132.5	58665.83471	12929.0
	58680.20956	5133.0	58669.30585	12930.0
	58681.29775	5133.5	–	–
39	59363.02430	5341.0	59362.71076	13129.5
	59364.12574	5341.5	59363.59784	13130.0
	59366.30682	5342.0	59367.06922	13131.0
	59367.40867	5342.5	59370.54086	13132.0
	59369.58978	5343.0	59373.12522	13132.5
	59370.69145	5343.5	59377.48376	13134.0
	59376.15546	5345.0	59380.06775	13134.5
	59377.25718	5345.5	59380.95529	13135.0
	59383.82263	5347.5	59383.53935	13135.5
	59386.00367	5348.0	59384.42653	13136.0
	59387.10551	5348.5	59387.01072	13136.5
66	60098.36333	5565.0	60116.00355	13346.5
	60099.47930	5565.5	60116.90441	13347.0
	60106.04501	5567.5	60119.47481	13347.5
	60108.21082	5568.0	60120.37585	13348.0
	60109.32776	5568.5	60123.84738	13349.0
	60111.49403	5569.0	–	–
	60124.62507	5573.0	–	–
	60125.74183	5573.5	–	–
93	60830.41946	5788.0	–	–
	60831.54999	5788.5	60831.11044	13552.5
	60833.70213	5789.0	60832.02502	13553.0
	60834.83282	5789.5	60834.58184	13553.5
	60836.98457	5790.0	60835.49652	13554.0
	60838.11565	5790.5	60838.05323	13554.5
	60840.26738	5791.0	60838.96796	13555.0
	60843.55052	5792.0	60844.99611	13556.5
	60844.68140	5792.5	60845.91089	13557.0
	60846.83317	5793.0	60848.46745	13557.5
	60847.96430	5793.5	60849.38236	13558.0
	60851.24705	5794.5	60851.93893	13558.5
	60853.39881	5795.0	60852.85381	13559.0
	60854.52982	5795.5	–	–